DOI: 10.1021/ma1019279

Macromolecules
ARTICLE

Micelle/Inverse Micelle Self-Assembly of a PEO−PNIPAm Block Copolymer in Ionic Liquids with Double Thermoresponsivity

Hau-Nan Lee,[†] Zhifeng Bai,[†] Nakisha Newell,[‡] and Timothy P. Lodge*[,†,‡]

[†]*Department of Chemistry and* [‡]*Department of Chemical Engineering and Materials Science, University of Minnesota, Minneapolis, Minnesota 55455, United States*

Received August 20, 2010; Revised Manuscript Received October 1, 2010

ABSTRACT: We report a doubly thermoresponsive diblock copolymer that exhibits both an upper critical micellization temperature (UCMT) and a lower critical micellization temperature (LCMT) in ionic liquids. Dynamic light scattering and cloud point measurements are employed to investigate the micellization behavior of poly(ethylene oxide)-*b*-poly(*N*-isopropylacrylamide) (PEO−PNIPAm) in 1-ethyl-3-methylimidazolium tetrafluoroborate ([EMIM][BF_4]), 1-butyl-3-methylimidazolium tetrafluoroborate ([BMIM][BF_4]), and their blends. In a single ionic liquid solvent, at low and high temperatures, the block copolymer self-assembles into PNIPAm-core and PEO-core micelles, respectively. The core and corona of the micelles are reversibly switchable in response to the stimulus of temperature. Using [EMIM][BF_4]/[BMIM][BF_4] blends as solvents, both the UCMTs and LCMTs can be easily tuned over a wide range of temperature by varying the mixing ratio of the two ionic liquids. Depending on the relative positions of the UCMT and LCMT, two types of doubly thermoresponsive systems (micelle−unimer−inverse micelle and micelle−copolymer aggregates−inverse micelle) can be obtained.

Introduction

Recently, much attention has been focused on "smart" polymeric materials owing to their scientific interest and potential technological applications.[1,2] The notable feature of these systems is that they respond in a dramatic way (solubility, shape, volume, surface properties, etc.) to slight changes in their surrounding environment, such as temperature, pH, ionic strength, electric potential, and light. The appeal of these materials lies not only in the rapid and drastic changes in structures and physical properties but also in their reversibility.

For some applications, a physical stimulus such as temperature is preferable in order to increase the number of switching cycles. Thermoresponsive block copolymers offer high potential for applications including temperature sensors, thermoresponsive gels, actuators, and suspending agents for delivery systems. The thermosensitivity of these materials often relies on a sharp change in solubility upon heating or cooling; i.e., they exhibit either lower critical solution temperature (LCST) or upper critical solution temperature (UCST) phase behavior. A well-known example is a block copolymer of poly(ethylene oxide) and poly(*N*-isopropylacrylamide) (PEO−PNIPAm), which exhibits thermoresponsive micellization in water above the LCST of PNIPAm.[3,4] In order to develop a new polymer that responds to temperature in a way that precisely fits the need of the application, the ability to fine-tune the transition temperature is required. In principle, the LCST or UCST of a given polymer can be tuned by incorporating different amounts of solvatophilic or solvatophobic comonomers[5,6] or by adding solvatophilic or solvatophobic branches.[7−9] However, synthesizing a random or graft copolymer with targeted properties can be a cumbersome trial-and-error process, and it is difficult to actually fine-tune the transition temperature as desired.

The recent development of polymeric materials in ionic liquids (ILs) has generated lots of excitement.[10−13] ILs are often viewed as "green solvents" due to their extremely low volatility and chemical/thermal stability.[14] These properties make ILs ideal materials for use in open atmosphere over a wide range of temperature. Moreover, the properties of ILs can be readily manipulated for a given application by varying the chemical structures of the ions.[15] Only recently have there been reports of thermoresponsive polymers exhibiting an UCST such as PNIPAm[16] or a LCST such as poly(benzyl methacrylate) (PBnMA),[17,18] poly(ethyl glycidyl ether),[19] and PEO[20] in ILs. An important feature of these thermosensitive homopolymers is that the UCST or LCST can be adjusted by varying the chemical structures of the cations and anions,[20,21] or by blending different ILs,[20,21] without changing the chemical structure of the polymers. This offers great convenience for designing a polymeric material with targeted properties. The polymer/ILs systems that can undergo UCST or LCST phase transition have been applied to design cross-linked PNIPAm and PBnMA gels with thermosensitive swelling/shrinking behavior,[16,17] thermoreversible block copolymer ion gels with high ion conductivity and tunable gel temperatures,[22,23] and micelle shuttle systems[24] that are relevant to molecular storage, transport, and separation.

One challenge is to develop more "sophisticated" polymers that can respond to more than one temperature change.[25] An example is an AB block copolymer where the A block has an LCST and the B block has a UCST, and thus it can form either A-core micelles or B-core micelles over two different temperature ranges in a single solvent. One potential application of a multithermoresponsive system is a sensor that can monitor different temperature ranges by adjusting the LCMT and UCMT of the material. In aqueous solution, there have been several reports of micelle/inverse micelle self-assembly systems that are triggered by temperature.[26−30] However, so far there is only one report of a doubly thermosensitive polymer in ILs.[31] Ueki et al. prepared a diblock copolymer consisting of an LCST PBnMA block and a UCST PNIPAm block that exhibits a thermally triggered micelle−unimer−inverse micelle transition. They also demonstrated that the UCMT could be altered by copolymerization of acrylamide in the PNIPAm block as well as by using different ILs as solvents.

In this paper, we report a novel doubly thermoresponsive PEO−PNIPAm diblock copolymer that exhibits both UCMT

*Author for correspondence: e-mail lodge@umn.edu.

 Published on Web 10/21/2010

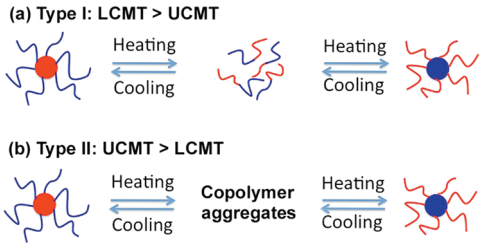

Figure 1. Schematic illustration of two types of doubly thermosensitive self-assembly of PEO−PNIPAm in ionic liquid blends. The red and blue blocks represent PNIPAm and PEO blocks, respectively. (a) LCMT > UCMT: micelle−unimer−inverse micelle self-assembly. (b) UCMT > LCMT: micelle−copolymer aggregates−inverse micelle self-assembly.

and LCMT behavior in 1,3-dialkylimidazolium tetrafluoroborate ILs. The molecular design of the thermoresponsive system is based on the LCST of PEO[20] and the UCST of PNIPAm[16] in ILs. The core and corona of micelles are reversibly switchable in response to changes in temperature. A well-defined PEO−PNIPAm block copolymer was prepared by reversible addition−fragmentation chain transfer (RAFT) polymerization. The micellization behavior of PEO−PNIPAm in 1-ethyl-3-methylimidazolium tetrafluoroborate ([EMIM][BF_4]), 1-butyl-3-methylimidazolium tetrafluoroborate ([BMIM][BF_4]), and their blends was studied using dynamic light scattering (DLS) and cloud point (CP) measurements. The nonvolatility and good thermostability of ILs allow us to investigate the micellization behavior from room temperature up to 230 °C.

We find that, using [EMIM][BF_4]/[BMIM][BF_4] blends as solvents, the LCST of PEO and the UCST of PNIPAm decreases and increases, respectively, as the weight fraction of [EMIM][BF_4] in the IL blends increases. Therefore, both UCMTs and LCMTs of PEO−PNIPAm/ILs systems can be easily tuned over a wide range of temperatures by simply varying the mixing ratio of two ILs, without modifying the chemical structure of the copolymer. As shown in Figure 1, two types of doubly reversible thermoresponsive system (micelle−unimer−inverse micelle and micelle−copolymer aggregates−inverse micelle) can be obtained by appropriately adjusting the mixing ratio of IL blends. For both types of systems, at low and high temperatures, the block copolymer self-assembles into PNIPAm-core and PEO-core micelles, respectively. However, at intermediate temperatures, depending on the relative positions of the UCMT and LCMT, the block copolymer is either soluble or insoluble.

Experimental Section

Materials. Hydroxy-terminated PEO-20 (the number indicates the molecular weight in kg/mol) homopolymer with a polydispersity of 1.14 was purchased from Aldrich. PNIPAm-40 homopolymer with a polydispersity of 1.70 was purchased from Polysciences. The glass transition temperatures (T_g) of PEO-20 and PNIPAm-40 are −46 and 109 °C, respectively, as determined from a TA Instruments Q1000 DSC at a heating rate of 10 °C/min. [EMIM][BF_4] and [BMIM][BF_4] were synthesized via the procedures described in a previous publication.[20] Both ILs were used after drying in a vacuum oven at 50 °C for at least 2 days. The temperature-dependent viscosity of [EMIM][BF_4] was measured on an Advanced Rheometric Expansion System (ARES) rheometer (see Supporting Information for details). The temperature-dependent viscosity of [BMIM][BF_4] was obtained from the literature.[32] The refractive indices of [EMIM][BF_4] and [BMIM][BF_4] are 1.418 and 1.424, respectively, as measured by an Abbe refractometer at 488 nm. The viscosities and refractive indices of [EMIM][BF_4]/[BMIM][BF_4] blends were calculated from linear interpolation based on the molar ratio between two ILs, assuming ideal mixing behavior.

The materials used to prepare the PEO−PNIPAm diblock copolymer are as follows. PEO methyl ether (M_n = 19 000, M_w/M_n = 1.08) was purchased from Polymer Source and purified by precipitation in *n*-hexane. The chain transfer agent (CTA) *S*-1-dodecyl-*S*′-(α,α′-dimethyl-α′′-acetic acid) trithiocarbonate was synthesized following a reported procedure.[33] NIPAm monomer and 2,2′-azobis(isobutyronitrile) (AIBN) were purchased from Aldrich and purified by recrystallization from benzene/*n*-hexane (65/35 v/v) and methanol, respectively. All the other chemicals and solvents were obtained from Aldrich and used as received.

RAFT Polymerization of PEO−PNIPAm. The PEO−PNIPAm block copolymer was synthesized following a procedure reported previously.[23,24] In brief, the hydroxyl end group of PEO methyl ether was first coupled to a chain transfer agent (CTA) via an acid chloride intermediate to form a PEO−CTA macroinitiator. The PEO−CTA was subsequently used to grow PNIPAm blocks via RAFT polymerization. The size exclusion chromatography (SEC) curve (Figure S2) of the PEO−PNIPAm copolymer shows an additional peak located at the lower molecular weight end, indicating the formation of trace amount of PNIPAm homopolymer during the RAFT polymerization. After washing with ethanol several times, the additional peak disappears (Figure S2); the fraction of remaining PNIPAm homopolymer is lower than the detection limit of the SEC. The purified polymer has a 19 kDa PEO block and a 12 kDa PNIPAm block as determined by ^{1}H NMR spectroscopy and a polydispersity of M_w/M_n = 1.16 as determined by SEC.

Preparation of Polymer/ILs Solutions. A strict procedure was applied to prepare polymer/ILs solutions for CP and DLS measurements to minimize water and cosolvent content. PEO/ILs solutions were prepared by mixing the polymer and ILs in ampules and stirring at ∼80 °C under vacuum (< 50 mTorr) until complete dissolution. The solutions were continuously stirred under vacuum at 80 °C for at least 18 h to completely remove any residual moisture and then were flame-sealed in an argon atmosphere to prevent moisture and degradation of components at high temperatures. A cosolvent method was used to prepare PNIPAm/IL solutions. PNIPAm and ILs were first dissolved in an ampule with the assistance of dichloromethane. The dichloromethane was then slowly evaporated under the purge of nitrogen followed by drying under vacuum (< 50 mTorr) for at least 40 h to remove the cosolvent. Finally, the ampules were flame-sealed in an argon atmosphere. The same cosolvent method was applied to prepare PEO−PNIPAm micelle solutions for the DLS measurements. After the removal of the cosolvent, the micelle solutions were passed through 0.45 μm syringe filters into DLS glass tubes with an inner diameter of 0.2 in., and the tubes were then flame-sealed under vacuum to prevent moisture and degradation.

Cloud Point Measurements. The CPs of PEO/IL (LCST) and PNIPAm/IL (UCST) were determined by optical transmittance measurements at 632.8 nm at a heating and cooling rate of roughly 1 °C/min, respectively. The solution was placed in a temperature-controlled oil bath. The temperature dependence of transmittance was monitored using a laser power detector (SPEX) while the solution was stirred. We define the CP values as the temperatures at which the transmittance drops to 80%.

A different heating protocol was applied to determine the CPs for PEO−PNIPAm/IL solutions that are insoluble at intermediate temperatures. A heating rate of ∼1 °C/min was first used until the temperature exceeded the LCMT. After that, much slower heating was used. The transmittance was measured every 1−5 °C, and before each measurement, the solution was allowed to equilibrate at each temperature for 30 min.

Dynamic Light Scattering Measurements. The details of DLS measurements and the data analysis procedure can be found elsewhere.[10,34] A home-built instrument equipped with a Brookhaven BI-DS photomultiplier mounted onto a goniometer, a Lexel Ar^+ laser operating at 488 nm, and a Brookhaven BI-9000 correlator was used to perform the DLS measurements. In a typical DLS measurement, the sample tube was first placed in a temperature-controlled index-matching oil bath for 20 min or

until a steady scattering intensity was observed (up to several hours for some measurements). The intensity correlation function, $g_2(q,t)$, was then measured at a fixed 90° scattering angle. The accumulation time for measuring $g_2(q,t)$ ranged from 600 to 1200 s.

The measured $g_2(q,t)$ were then transformed to the electric field autocorrelation functions, $g_1(q,t)$, using the Siegert relation,[35] $g_2(q,t) - 1 = g_1^2(q,t)$. The resulting $g_1(q,t)$ functions were analyzed using the method of cumulants[36] to evaluate the average decay rate, $\bar{\Gamma}$, and the width of the decay, $\mu_2/\bar{\Gamma}^2$.

$$g_1(q,t) = A\exp(-\bar{\Gamma}t)\left(1+\frac{1}{2!}\mu_2 t^2+\ldots\right) \quad (1)$$

The average decay rate, $\bar{\Gamma}$, was used to calculate the mutual diffusion coefficients, $D_m = \bar{\Gamma}/q^2$, where q is the scattering vector defined as $q = (4\pi n/\lambda_0)\sin(\theta/2)$, n is the refractive index of the solvent, λ_0 is the wavelength of the light in vacuum, and θ is the scattering angle. In the limit of low concentration, D_m can be approximated by the tracer diffusion coefficient, D_t, and the hydrodynamic radii of micelles can be extracted through the Stokes−Einstein equation

$$R_h = \frac{k_B T}{6\pi\eta D_t} \quad (2)$$

where k_B is the Boltzmann constant, T is the temperature, and η is the viscosity of the solvent.

The distribution of hydrodynamic radius was obtained by applying an inverse Laplace transformation to the $g_1(q,t)$ function.[37] When the size distribution displayed a bimodal distribution, the $g_1(q,t)$ function was fit to a double-exponential function to extract the average decay rates from the two distinct distributions.

$$g_1(t) = A_1\exp(-\bar{\Gamma}_1 t) + A_2\exp(-\bar{\Gamma}_2 t) + B \quad (3)$$

Results and Discussion

LCST of PEO and UCST of PNIPAm in IL Blends. In a recent publication, Lee and Lodge reported the LCST-type liquid−liquid phase behavior of PEO in [EMIM][BF_4] and [BMIM][BF_4].[20] They also found unusual temperature−composition phase diagrams in which the CP curves are strongly asymmetric, with the critical composition shifted to high concentrations of PEO. In these PEO/IL systems, the molecular weight of PEO does not have a strong influence on the phase behavior. In addition, as shown in Figure 2, the IL structure has a significant influence on the miscibility of a PEO/IL solution. A small decrease in the alkyl chain length ($C_4 \rightarrow C_2$) in the imidazolium cation results in a ~45 °C decrease in the phase transition temperature. More importantly, the CP values decrease almost linearly from 209 °C for [BMIM][BF_4] to 163 °C for [EMIM][BF_4] as the weight fraction of [EMIM][BF_4] increases, indicating that the value of LCST can be easily controlled by appropriately adjusting the mixing ratio of two ILs.

The LCST phase behavior was also observed for PEO-20 in 1-ethyl-3-methylimidazolium bromide/1-ethyl-3-methylimidazolium bis{(trifluoromethyl)sulfonyl}amide ([EMIM][Br]/[EMIM][TFSA]) blends, and as shown in Figure S3, a similar linear trend was also obtained.

Ueki and Watanabe have reported the UCST phase behavior of PNIPAm in an IL.[16] They also found that the molecular weight of PNIPAm does not have strong influence on the phase behavior, and the CP increases as the weight fraction of PNIPAm in IL increases from 1 wt % up to 10 wt %. To tune the

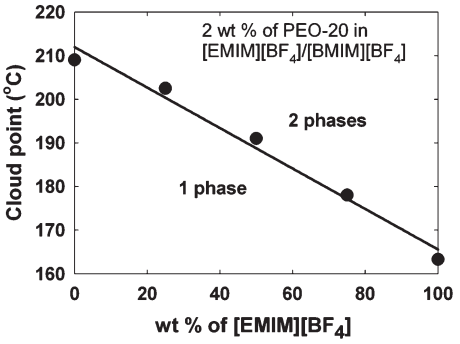

Figure 2. Cloud point values for 2 wt % PEO-20 in [EMIM][BF_4]/[BMIM][BF_4] blends. The solid line is a linear fit to the data. The data points are obtained from ref 20.

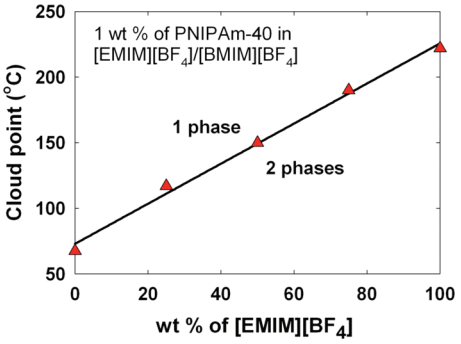

Figure 3. Cloud point values for 1 wt % PNIPAm-40 in [EMIM][BF_4]/[BMIM][BF_4] blends. The solid line is a linear fit to the data.

UCST of PNIPAm, we use [EMIM][BF_4]/[BMIM][BF_4] blends as solvents. Figure 3 shows the CP values of 1 wt % PNIPAm-40 in IL blends as a function of the weight fraction of [EMIM][BF_4]. To determine the CP, the solution was first heated above the transition temperature and stirred until complete dissolution. The temperature-dependent transmittance was then measured at a cooling rate of roughly 1 °C/min. This UCST phase transition is completely reversible. The IL structure has a substantial impact on the miscibility of a PNIPAm/IL solution. A decrease in the alkyl chain length ($C_4 \rightarrow C_2$) in the imidazolium cation results in a ~155 °C increase in the UCST. Similar to the linear change shown in Figure 2, the CP values increase almost linearly as the weight fraction of [EMIM][BF_4] increases. The value of the CP can be easily tuned between 67 and 222 °C by appropriately adjusting the mixing ratio of two ILs. This linearity was also observed for the CPs of PNIPAm in 1-ethyl-3-methylimidazolium bis{(trifluoromethyl) sulfonyl}amide/1-butyl-3-methylimidazolium hexafluorophosphate ([EMIM][TFSA]/[BMIM][PF_6]) blends (Figure S4).

The observation of linearity for both PEO/ILs and PNIPAm/ILs system is consistent with the LCST phase behavior of PBnMA in [EMIM][TFSA]/[BMIM][TFSA] blends studied by Watanabe and co-workers.[21] It is likely that this linearity can be generally observed in any polymer/IL system with a critical phase behavior, where the ionic liquid components are similar. In contrast, this linearity is not typical in polymer/molecular solvent systems. For example, Schild, Muthukumar, and Tirrell[38] showed that the LCST of PNIPAm first decreases and then increases as the fraction of organic solvent (methanol, THF, or dioxane) in water increases. This linear trend of UCST or LCST in polymer/ILs suggests that mixing two different ionic liquids does not change the nature of the interactions between polymer and ions very much. Therefore, it is an ideal random mixing process, as expected.

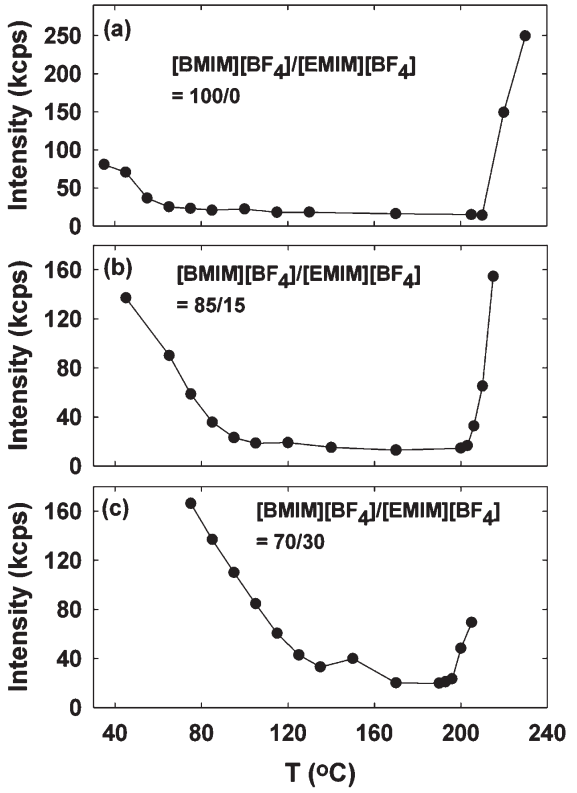

Figure 4. Temperature dependence of scattering intensity for 1 wt % PEO−PNIPAm in (a) $[BMIM][BF_4]$, (b) 85/15 $[BMIM][BF_4]$/$[EMIM][BF_4]$ blends, and (c) 70/30 $[BMIM][BF_4]$/$[EMIM][BF_4]$ blends.

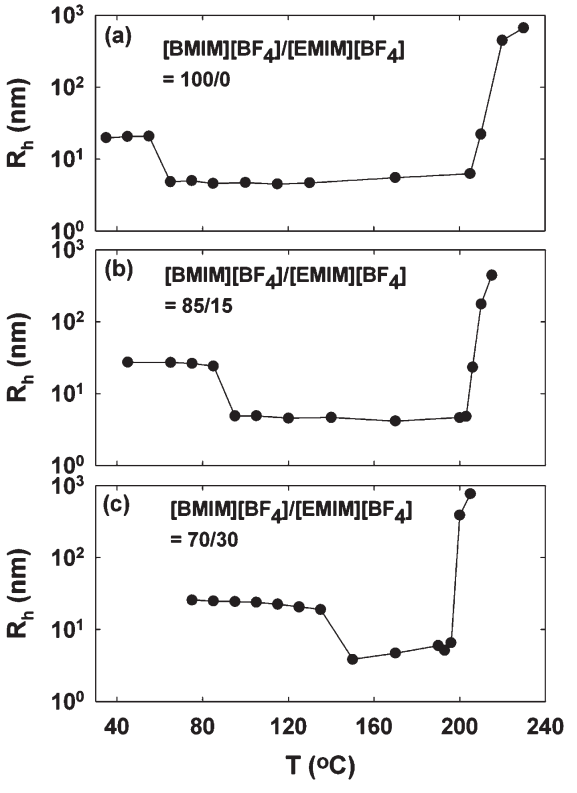

Figure 5. Temperature dependence of hydrodynamic radius (R_h) for 1 wt % PEO−PNIPAm in (a) $[BMIM][BF_4]$, (b) 85/15 $[BMIM][BF_4]$/$[EMIM][BF_4]$ blends, and (c) 70/30 $[BMIM][BF_4]$/$[EMIM][BF_4]$ blends.

Micellization of PEO−PNIPAm Diblock Copolymer in IL Blends. Type I: LCMT > UCMT. On the basis of the LCST of PEO and the UCST of PNIPAm, we designed a doubly thermosensitive PEO−PNIPAm diblock copolymer synthesized via RAFT polymerization. Dynamic light scattering was employed to investigate the micellization of the block copolymer in IL blends. Figure 4a shows the scattering intensity at $\theta = 90°$ as a function of temperature from a 1 wt % PEO−PNIPAm in $[BMIM][BF_4]$. Low levels of scattering intensity indicate molecular dissolution, and increased scattering intensity indicates the formation of micelles. The result suggests that, in $[BMIM][BF_4]$, PEO−PNIPAm self-assembles into micelles at low and high temperatures and dissolves at intermediate temperatures.

Figure 5a displays the corresponding mean hydrodynamic radius (R_h) as a function of temperature for 1 wt % PEO−PNIPAm in $[BMIM][BF_4]$. At low and high temperatures, R_h is determined from cumulant analysis. In the intermediate temperature range, R_h is obtained from a double-exponential fit; only the smaller values are plotted, since large aggregates in this temperature range represent a very small fraction (see below for details). Both scattering intensity (Figure 4a) and hydrodynamic radius (Figure 5a) results indicate that there are two distinct transition temperatures located at ~60 °C (UCMT) and ~207 °C (LCMT), near the CPs of PNIPAm and PEO, respectively. Therefore, we conclude that the block copolymers form PNIPAm-core and PEO-core micelles at low and high temperatures, respectively, as illustrated in Figure 1a.

Figure 6 shows selected distributions of the hydrodynamic radius at 35, 130, and 230 °C for PEO−PNIPAm in $[BMIM][BF_4]$. As shown in panels a and c, monomodal distributions at low and high temperatures clearly indicate the formation of well-defined micelles. However, at intermediate temperatures,

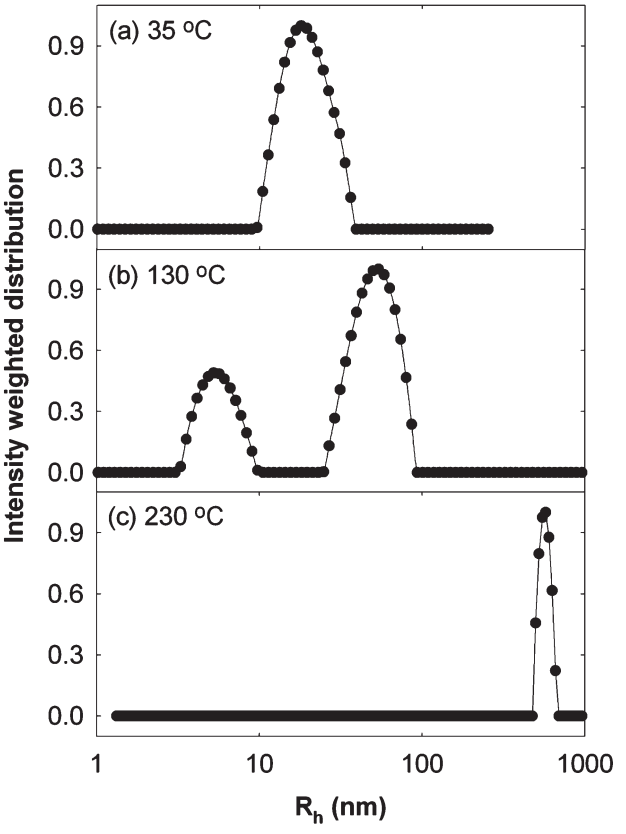

Figure 6. Intensity-weighted hydrodynamic radius distribution for 1 wt % PEO−PNIPAm in $[BMIM][BF_4]$ at (a) 35 °C (micelles with PNIPAm core and PEO corona), (b) 130 °C (unimers with trace amount of aggregates), and (c) 230 °C (micelles with PEO core and PNIPAm corona).

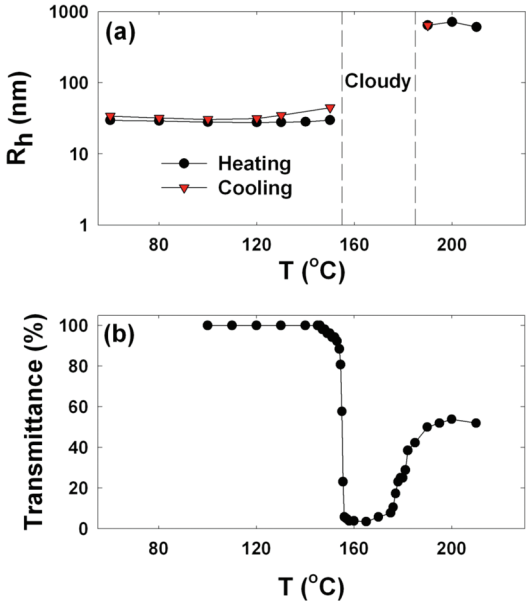

Figure 7. Micellization of 1 wt % PEO−PNIPAm in 50/50 [BMIM]-[BF_4]/[EMIM][BF_4] blends: (a) hydrodynamic radius obtained from DLS measurements; (b) transmittance at 632.8 nm. The solution becomes cloudy between 155 and 185 °C.

the size distribution always displayed a bimodal distribution (panel b). The small R_h peak corresponds to single polymer chains, whereas the large R_h peak indicates the existence of large aggregates. These aggregates may arise from the tiny fraction of polymers with very high molecular weight that are reluctant to dissolve. Given that the overall scattering intensity at intermediate temperatures is very low (Figure 4a) and the scattering intensity is roughly proportional to R_h^6 (Rayleigh approximation), the number fraction of single polymer chains at this temperature is estimated to be more than 99.9%.

Selected DLS measurements at a few temperatures during both cooling and reheating processes were performed to check the reversibility. The results indicate that this micelle−unimer−inverse micelle phase transition is rapid (the scattering intensity reaches a steady value in less than 10 min) and completely reversible, even after heating up to 230 °C.

Figure 4b,c shows the temperature-dependent scattering intensity for 1 wt % PEO−PNIPAm in 85/15 [BMIM][BF_4]/[EMIM][BF_4] and 70/30 [BMIM][BF_4]/[EMIM][BF_4] blends, respectively. The corresponding temperature-dependent hydrodynamic radii are shown in Figure 5b,c. In both IL blends, two distinct phase transition temperatures can be identified, indicating the existence of micelle−unimer−inverse micelle phase transition behavior. Similar to the LCSTs and UCSTs of homopolymer/ILs systems, the UCMTs and LCMTs of the copolymer/ILs systems increase and decrease, respectively, as the weight fraction of [EMIM][BF_4] increases. This result indicates that the values of LCMT and UCMT can also be tuned by appropriately adjusting the mixing ratio of two ILs.

For all three copolymer/ILs systems shown in Figures 4 and 5, the R_h of the PNIPAm-core micelles at low temperatures are around 25 nm, while the R_h of the PEO-core micelles at high temperatures are on the order of several hundred nanometers. The size of the PEO-core micelles is significantly larger than that of the PNIPAm-core micelles, suggesting that the structures of the two micelles are different. The numbers of repeat units in the PNIPAm and PEO blocks are ∼105 and ∼430, respectively. Considering the length difference between two blocks, it is probable that, at

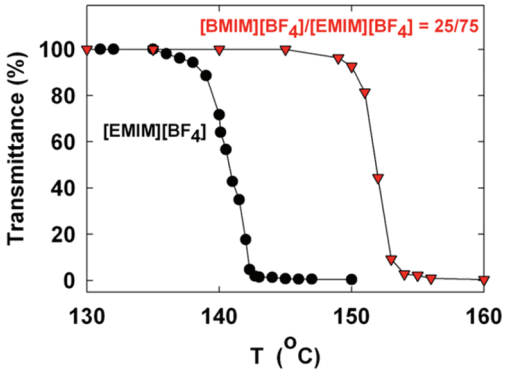

Figure 8. Temperature dependence of transmittance at 632.8 nm for 1 wt % PEO−PNIPAm in [EMIM][BF_4] and 25/75 [BMIM][BF_4]/[EMIM]-[BF_4] blends.

low temperatures, the copolymers self-assemble into spherical micelles with PNIPAm-cores. However, at high temperatures, the copolymers may self-assemble into wormlike micelles or vesicles with PEO-cores.

Micellization of PEO−PNIPAm in IL Blends. Type II: UCMT > LCMT. Further increase in the weight fraction of [EMIM][BF_4] in the IL blends transforms the solution into a different type of doubly thermosensitive system. Figure 7a shows the temperature-dependent hydrodynamic radius for 1 wt % PEO−PNIPAm in 50/50 [BMIM][BF_4]/[EMIM][BF_4] during both heating and cooling processes. The micellization of this copolymer/IL solution is similar to that of copolymer in [BMIM][BF_4]-rich IL blends (Figures 4 and 5): small size PNIPAm-core micelles and large size PEO-core micelles are observed at low and high temperatures, respectively. However, at intermediate temperatures (155−185 °C), the solution becomes cloudy, indicating the occurrence of phase separation. This observation suggests that, in this copolymer/ILs system, the LCMT is lower than the UCMT. Heating above the LCMT likely causes the PEO corona to collapse, and separate micelles coalesce to form aggregates. Consequently, as the temperature increases, the solution undergoes micelle−aggregates−inverse micelle transitions, as illustrated in Figure 1b. Note that, although it undergoes a rapid (∼10 min) PNIPAm-core micelle to copolymer aggregate transition upon heating, it takes at least 3 h for a turbid aggregate solution to turn into a PEO-core micelle solution. Similarly, upon cooling, a rapid micelle-to-aggregates transition is observed, but it takes more than 12 h for the aggregates to dissociate into stable micelles.

The thermally induced phase transition of PEO−PNIPAm in 50/50 [BMIM][BF_4]/[EMIM][BF_4] was also investigated using transmittance measurements. A different heating protocol was employed for this measurement. A heating rate of ∼1 °C/min was first applied until the temperature reaches 175 °C (above the LCMT). After that, a much slower heating method was applied; the solution was allowed to equilibrate at each temperature for 30 min before performing a transmittance measurement. Consistent with the results of DLS, as shown in Figure 7b, high transmittance is observed at low temperatures followed by a drastic decrease in the transmittance at ∼155 °C, indicating a sharp LCMT-type phase transition. A turbid solution is obtained between 155 and 185 °C. Further increase in the solution temperature leads to an increase in the transmittance at ∼185 °C, suggesting the presence of UCMT-type phase transition. Cooling the solution makes it turn cloudy and then slowly become transparent again. The same phase transitions are observed by repeating the heating and cooling processes. The UCMT phase transition is relatively broader than the LCMT phase

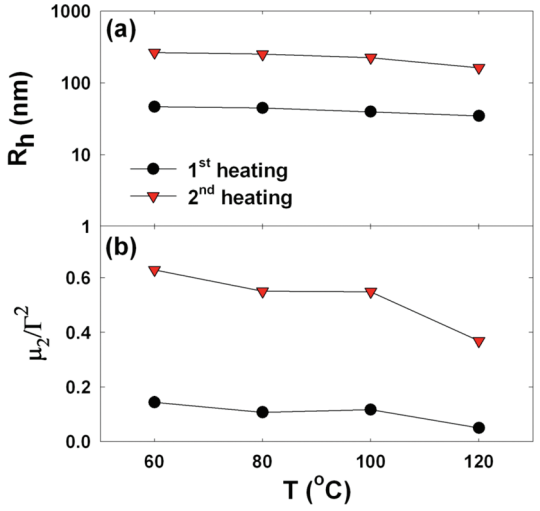

Figure 9. Micellization of 1 wt % PEO−PNIPAm in [EMIM][BF_4] investigated by DLS: (a) hydrodynamic radius and (b) reduced second cumulant $\mu_2/\bar{\Gamma}^2$. Data from two consecutive heating scans are presented. The solution was heated above the LCMT, annealed at 130 °C for more than 24 h, and then cooled to room temperature before the second heating scan.

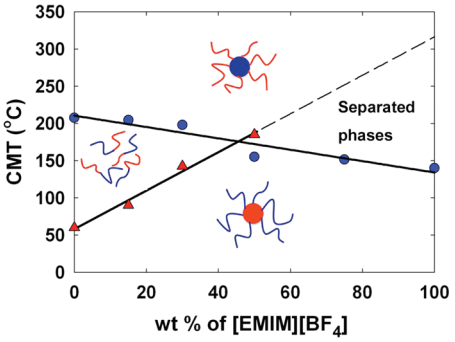

Figure 10. Phase diagram of 1 wt % of PEO−PNIPAm in [BMIM]-[BF_4]/[EMIM][BF_4] blends. The *x*-axis corresponds to the weight fraction of [EMIM][BF_4] in the IL blends. The blue circles and red triangles are values of LCMT and UCMT, respectively, as determined by DLS and transmittance measurements shown in Figures 4, 5, 7, and 8. The lines that divide the phase diagram into four regions are linear fits to the data. The cartons illustrate the morphologies of PEO−PNIPAm copolymer in different regions of phase diagram. The red and blue blocks represent PNIPAm and PEO blocks, respectively.

transition. This is likely due to a kinetic effect. The formation of micelles from copolymer aggregates heated across the UCMT is similar to a direct dissolution process. It is generally observed that direct dissolution method requires longer time to form a narrow distribution of micelles.[34,39]

Figure 8 shows the results of transmittance measurements for 1 wt % PEO−PNIPAm in two [EMIM][BF_4]-rich IL blends. Consistent with the CPs of PEO in IL blends shown in Figure 2, further increase in the weight fraction of the [EMIM][BF_4] in IL blends leads to a decrease in the value of the LCMT. The LCMTs of 1 wt % PEO−PNIPAm in 25/75 [BMIM][BF_4]/[EMIM][BF_4] blends and pure [EMIM][BF_4] are determined as 151.5 and 140 °C, respectively. However, after the phase separation, both solutions remain cloudy up to 230 °C; no additional phase transition is observed. It is likely that the UCMTs of these two systems are higher than 230 °C, i.e., higher than the limit of our measurements. Degradation of block copolymer and/or ILs occurs after holding at temperatures above 240 °C for more than 10 min, as evidenced from the formation of a yellowish gel-like material. The LCMTs of PEO−PNIPAm in these two [EMIM]-[BF_4]-rich ILs are noticeably lower than the LCSTs of PEO in the same ILs. Attaching an insoluble PNIPAm block to a PEO block makes the PEO block less soluble in ILs.

An experiment to check the reversibility of the phase transition for PEO−PNIPAm in [EMIM][BF_4] yields an interesting result that is different from the observations of PEO−PNIPAm in [BMIM][BF_4]-rich IL blends. Figure 9 shows the temperature dependence of R_h and $\mu_2/\bar{\Gamma}^2$ for the as-prepared solution (first heating) and the solution after undergoing a phase separation (second heating). Before the second heating scan, the solution was annealed at 130 °C (below the LCMT) for more than 24 h until a steady scattering intensity was obtained. The morphologies of micelles obtained during the first and second heating scans are significantly different; R_h measured during the first heating are about 5 times smaller, and the values of $\mu_2/\bar{\Gamma}^2$ are much smaller, indicating a narrower size distribution of micelles. The subsequent cooling/reheating cycles yield the similar R_h and $\mu_2/\bar{\Gamma}^2$ as those measured during the second heating.

The structural difference between the first and second heating experiments may be due to the difference in micellar formation processes. In a recent study,[34,39] Meli and Lodge showed that different preparation protocols for the same copolymer and ionic liquid can generate micelles with substantially different sizes. They found that poly((1,2-butadiene)-block-ethyleneoxide) (PB−PEO) micelles prepared by a cosolvent method have smaller R_h and narrower size distribution. In contrast, micelles prepared by a direct dissolution method have larger R_h and broader size distribution. They also found that, after annealing the micelle solutions prepared by direct dissolution method at 170 °C (~180 °C higher than the T_g of the insoluble PB core) for a few hours, the micelles reach a steady state with a smaller R_h and a narrower distribution. In our experiments, the micelles observed during the first heating scan are initially formed with the assistance of molecular cosolvent. On the other hand, the micelles observed during the second heating and the subsequent cooling/reheating are formed from copolymer aggregates cooled across the LCMT. The mechanism causing the difference in micellar morphology is not yet clear. However, the micelles obtained from copolymer aggregates cooled across the LCMT may be similar to a direct dissolution process. Before the second heating scan, we annealed the sample at 130 °C; that is only ~25 °C higher than the T_g of the insoluble PNIPAm core. It is likely that the relaxation of micelles at this temperature is too slow so that the system has not reached a steady state. Therefore, a larger R_h and a wider size distribution were observed.

PEO−PNIPAm/IL Blends Phase Diagram. Figure 10 illustrates a PEO−PNIPAm/ILs phase diagram constructed from the LCMT and UCMT data determined from DLS and transmittance measurements shown in Figures 4, 5, 7, and 8. The LCMT values decrease almost linearly from 210 °C for [BMIM][BF_4] to 134 °C for [EMIM][BF_4] as the weight fraction of [EMIM][BF_4] increases. Concurrently, the UCMT values increase almost linearly from 60 °C for [BMIM][BF_4] to 315 °C for [EMIM][BF_4] (extrapolated value) as the weight fraction of [EMIM][BF_4] increases. This result indicates that the values and the relative positions of LCMT and UCMT can be easily controlled by appropriately adjusting the mixing ratio of two ILs, without modifying the chemical structure of the polymer.

The two LCMT and UCMT lines divide the phase diagram into four regions. In IL blends with lower weight fraction of [EMIM][BF_4] (left-hand side of the diagram), the LCMTs are higher than the UCMTs. In this regime, the morphology of PEO−PNIPAm copolymer can change from PNIPAm-core micelles to unimers and then to PEO-core micelles as temperature increases (Figure 1a). On the other

hand, in IL blends with higher weight fraction of [EMIM][BF_4] (right-hand side of the diagram), the UCMTs are higher than the LCMTs. In this regime, a different type of dual thermosensitive micellization is obtained; copolymer undergoes a micelle−aggregates−inverse micelle phase transition as temperature increases (Figure 1b).

Conclusions

On the basis of the LCST of PEO and the UCST of PNIPAm in ILs, we designed a PEO−PNIPAm copolymer via RAFT polymerization that exhibits doubly thermosensitive self-assembly. DLS and transmittance measurements reveal the complex micellization behavior of PEO−PNIPAm in ILs. The block copolymer forms PNIPAm-core micelles at low temperatures and transforms to PEO-core micelles at high temperatures; this micelle/inverse micelle transition is reversible. The nonvolatility, stability, and tunability of ILs allow us to adjust both UCMT and LCMT values over a wide range of temperature simply by varying the mixing ratio of two ILs. This work demonstrates the flexibility of block copolymers for controlling nanostructure in ILs and offers potential opportunity for designing a new thermosensitive material.

Acknowledgment. This work was supported by the National Science Foundation (DMR-0804197). The support of the NSF-REU program (DMR-075492) at the University of Minnesota MRSEC (N.N.) and a Frieda Martha Kunze Fellowship (Z.B.) is also appreciated.

Supporting Information Available: Figures showing viscosity of [EMIM][BF_4], SEC traces of PEO−PNIPAm copolymer, LCST of PEO-20 in [EMIM][Br]/[EMIM][TFSA], and UCST of PNIPAm-25 in [EMIM][TFSA]/[BMIM][PF_6]. This material is available free of charge via the Internet at http://pubs.acs.org.

References and Notes

(1) Stuart, M. A. C.; Huck, W. T. S.; Genzer, J.; Muller, M.; Ober, C.; Stamm, M.; Sukhorukov, G. B.; Szleifer, I.; Tsukruk, V. V.; Urban, M.; Winnik, F.; Zauscher, S.; Luzinov, I.; Minko, S. *Nature Mater.* **2010**, *9*, 101–113.
(2) Liu, F.; Urban, M. W. *Prog. Polym. Sci.* **2010**, *35*, 3–23.
(3) Topp, M. D. C.; Dijkstra, P. J.; Talsma, H.; Feijen, J. *Macromolecules* **1997**, *30*, 8518–8520.
(4) Topp, M. D. C.; Leunen, I. H.; Dijkstra, P. J.; Tauer, K.; Schellenberg, C.; Feijen, J. *Macromolecules* **2000**, *33*, 4986–4988.
(5) Takei, Y. G.; Aoki, T.; Sanui, K.; Ogata, N.; Okano, T.; Sakurai, Y. *Bioconjugate Chem.* **1993**, *4*, 341–346.
(6) Rackaitis, M.; Strawhecker, K.; Manias, K. *J. Polym. Sci., Part B: Polym. Phys.* **2002**, *40*, 2339–2342.
(7) Virtanen, J.; Baron, C.; Tenhu, H. *Macromolecules* **2000**, *33*, 336–341.
(8) Bokias, G.; Hourdet, D.; Iliopoulos, I. *Macromolecules* **2000**, *33*, 2929–2935.
(9) Laschewsky, A.; Rekai, E. D.; Wischerhoff, E. *Macromol. Chem. Phys.* **2001**, *202*, 276–286.
(10) He, Y. Y.; Li, Z. B.; Simone, P.; Lodge, T. P. *J. Am. Chem. Soc.* **2006**, *128*, 2745–2750.
(11) Ueki, T.; Watanabe, M. *Macromolecules* **2008**, *41*, 3739–3749.
(12) Lodge, T. P. *Science* **2008**, *321*, 50–51.
(13) Lu, J. M.; Yan, F.; Texter, J. *Prog. Polym. Sci.* **2009**, *34*, 431–448.
(14) Rogers, R. D.; Seddon, K. R. *Science* **2003**, *302*, 792–793.
(15) Hough, W. L.; Smiglak, M.; Rodriguez, H.; Swatloski, R. P.; Spear, S. K.; Daly, D. T.; Pernak, J.; Grisel, J. E.; Carliss, R. D.; Soutullo, M. D.; Davis, J. H.; Rogers, R. D. *New J. Chem.* **2007**, *31*, 1429–1436.
(16) Ueki, T.; Watanabe, M. *Chem. Lett.* **2006**, *35*, 964–965.
(17) Ueki, T.; Watanabe, M. *Langmuir* **2007**, *23*, 988–990.
(18) Ueki, T.; Arai, A. A.; Kodama, K.; Kaino, S.; Takada, N.; Morita, T.; Nishikawa, K.; Watanabe, M. *Pure Appl. Chem.* **2009**, *81*, 1829–1841.
(19) Tsuda, R.; Kodama, K.; Ueki, T.; Kokubo, H.; Imabayashi, S.; Watanabe, M. *Chem. Commun.* **2008**, 4939–4941.
(20) Lee, H. N.; Lodge, T. P. *J. Phys. Chem. Lett.* **2010**, *1*, 1962–1966.
(21) Kodama, K.; Nanashima, H.; Ueki, T.; Kokubo, H.; Watanabe, M. *Langmuir* **2009**, *25*, 3820–3824.
(22) He, Y. Y.; Lodge, T. P. *Macromolecules* **2008**, *41*, 167–174.
(23) He, Y. Y.; Lodge, T. P. *Chem. Commun.* **2007**, 2732–2734.
(24) Bai, Z. F.; He, Y. Y.; Young, N. P.; Lodge, T. P. *Macromolecules* **2008**, *41*, 6615–6617.
(25) Dimitrov, I.; Trzebicka, B.; Muller, A. H. E.; Dworak, A.; Tsvetanov, C. B. *Prog. Polym. Sci.* **2007**, *32*, 1275–1343.
(26) Arotcarena, M.; Heise, B.; Ishaya, S.; Laschewsky, A. *J. Am. Chem. Soc.* **2002**, *124*, 3787–3793.
(27) Virtanen, J.; Arotcarena, M.; Heise, B.; Ishaya, S.; Laschewsky, A.; Tenhu, H. *Langmuir* **2002**, *18*, 5360–5365.
(28) Weaver, J. V. M.; Armes, S. P.; Butun, V. *Chem. Commun.* **2002**, 2122–2123.
(29) Maeda, Y.; Mochiduki, H.; Ikeda, I. *Macromol. Rapid Commun.* **2004**, *25*, 1330–1334.
(30) Mori, H.; Kato, I.; Saito, S.; Endo, T. *Macromolecules* **2010**, *43*, 1289–1298.
(31) Ueki, T.; Watanabe, M.; Lodge, T. P. *Macromolecules* **2009**, *42*, 1315–1320.
(32) Tokuda, H.; Hayamizu, K.; Ishii, K.; Abu Bin Hasan Susan, M.; Watanabe, M. *J. Phys. Chem. B* **2004**, *108*, 16593–16600.
(33) Lai, J. T.; Filla, D.; Shea, R. *Macromolecules* **2002**, *35*, 6754–6756.
(34) Meli, L.; Santiago, J. M.; Lodge, T. P. *Macromolecules* **2010**, *43*, 2018–2027.
(35) Brown, W. *Dynamic Light Scattering: The Method and Some Applications*; Oxford University Press: New York, 1993.
(36) Koppel, D. E. *J. Chem. Phys.* **1972**, *57*, 4814–4820.
(37) Jakes, J. *Collect. Czech. Chem. Commun.* **1995**, *60*, 1781–1797.
(38) Schild, H. G.; Muthukumar, M.; Tirrell, D. A. *Macromolecules* **1991**, *24*, 948–952.
(39) Meli, L.; Lodge, T. P. *Macromolecules* **2009**, *42*, 580–583.